*Chemistry – A European Journal*

ChemEurJ Chemistry Europe European Chemical Societies Publishing

RESEARCH ARTICLE OPEN ACCESS

# The Palladium(IV)-Centered Hexatungstate Ion $[Pd^{IV}W_6O_{24}]^{8-}$

Pooja Kulashri[1] | Xiang Ma[1,2] | Mahmoud Elcheikh Mahmoud[1] | Bassem S. Bassil[1] | Talha Nisar[1,3] | Veit Wagner[1] | Samer Dawoud[4] | Laurent Ruhlmann[4] | Ulrich Kortz[1]

[1]School of Science, Campus Ring 1, Constructor University, Bremen, Germany | [2]Fujian Provincial Key Laboratory of Advanced Inorganic Oxygenated Materials, College of Chemistry, Fuzhou University, Fuzhou, Fujian, China | [3]Institute For Applied Materials – Ceramic Materials and Technologies, Karlsruhe Institute of Technology (KIT), Karlsruhe, Germany | [4]Institute of Chemistry (UMR Au CNRS n°7177), University of Strasbourg, Strasbourg, France

**Correspondence:** Ulrich Kortz (ukortz@constructor.university)

**Received:** 27 February 2026 | **Revised:** 12 May 2026 | **Accepted:** 14 May 2026

## ABSTRACT

We report on the synthesis of the palladium(IV)-containing hexatungstate $[Pd^{IV}W_6O_{24}]^{8-}$ (**$PdW_6$**) with a central 6-coordinated $Pd^{IV}$ ion, which is surrounded by a ring of six edge-shared $WO_6$ octahedra. The sodium salt of **$PdW_6$** was structurally characterized in the solid state by multiple techniques, and the solution redox chemistry was investigated by electrochemistry. The catalytic hydrogenation of *o*-xylene using supported **$PdW_6$** as a precatalyst was also studied.

## 1 | Introduction

Discrete metal-oxo anions comprising early *d*-block metal ions in high oxidation states (e.g., $Mo^{VI}$, $W^{VI}$, $V^{V}$), also called addenda, form a plethora of compounds known as polyoxometalates (POMs) [1–3]. Such structures are often based on $MO_6$ octahedra, which are shared by corners or edges (isopolyanions, e.g., $[V_{10}O_{28}]^{6-}$), and at times one or more additional (often tetrahedral) groups are present, resulting in heteropolyanions (e.g., $[(PO_4)W_{12}O_{36}]^{3-}$). POMs are usually isolated as salts, and many of them are water-soluble, although some salts can also be isolated that are soluble in organic solvents. Several elements in the periodic table can act as hetero groups, and some addenda sites can be replaced by many types of *p*, *d*, and *f*-block elements. Besides the enormous structural and compositional variety of POMs, their physiochemical properties attract much attention, such as reversible redox chemistry, solution stability, oxygen-rich surface, discrete analogues of metal-oxides, tunability of shape/size/composition/charge/solubility, magnetic, electrochemical, photochemical, and catalytic potential [4–6].

The class of noble metal-containing POMs is of particular interest, due to their promising catalytic activity [7, 8]. In particular, the number of structurally characterized palladium-containing POMs has been growing over the years. In 1994, Angus–Dunne reported $[Pd^{II}_2(W_5O_{18})_2]^{8-}$ comprising two square-planar-coordinated $Pd^{II}$ ions bridging two monovacant Lindqvist units $(W_5O_{18})^{6-}$ [9]. Between 2004 and 2011, our group reported a number of $Pd^{II}$-containing heteropolytungstates, such as $[Pd^{II}_2WO(H_2O)(A\text{-}\alpha\text{-}SiW_9O_{34})_2]^{12-}$ [10], $[Pd^{II}_3(\alpha\text{-}Sb^{III}W_9O_{33})_2]^{12-}$ [11], $[Pd^{II}_3(\alpha\text{-}As^{III}W_9O_{33})_2]^{12-}$ [12], $[Pd^{II}WO(H_2O)Na(\alpha\text{-}As^{III}W_9O_{33})_2]^{11-}$ [12], $[Pd^{II}_3(H_2O)_9Bi_2W_{22}O_{76}]^{8-}$ [13], $[Pd^{II}_2(\alpha\text{-}PW_{11}O_{39}H_{0.5})_2]^{9-}$ [14], $[Pd^{II}_2(\alpha_2\text{-}P_2W_{17}O_{61}H_n)_2]^{(16-2n)-}$ [14]. In 2012, Cronin's group reported some tungstoselenite and -tellurite derivatives, $[Pd^{II}_{10}Se^{IV}_{10}W_{52}O_{206}H_{12}]^{28-}$, $[Pd^{II}_{10}Se^{IV}_{10}W_{52}O_{206}H_{14}]^{26-}$, and $[Pd^{II}_6Te^{IV}_{19}W_{42}O_{190}]^{40-}$ [15]. Other examples include the Wells–Dawson derivatives $[Pd^{II}_4(P_2W_{15}O_{56})_2]^{15-}$ [16], and $[Pd^{II}_4(As_2W_{15}O_{56})_2]^{16-}$ [17], as well as $[Pd^{II}_4Se^{IV}_2W^{VI}_{14}O_{56}H]^{11-}$ and $[Pd^{II}_4Se^{IV}_4W^{VI}_{28}O_{108}H_{12}]^{12-}$ [18]. In 2018, Kortz's group reported on palladium(II) incorporation in the well-known cyclic $[As_4W_{40}O_{140}]^{28-}$ ion by isolating

Correction updated on 4th June 2026-Typographical errors have been updated in this version.

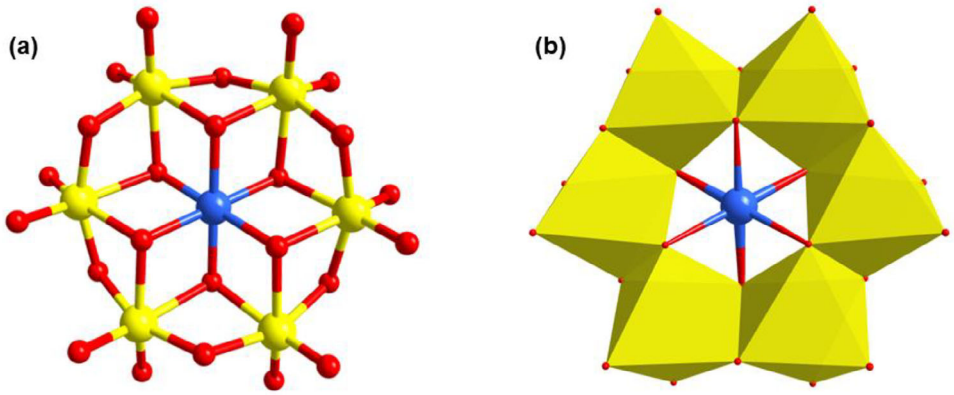


**FIGURE 1** | Structural representation of **$PdW_6$** (a) ball and stick representation. Color code: Pd (blue), W (yellow), and O (red). (b) polyhedral representation. Color code: Pd (blue), O (red), and $WO_6$ (yellow).

$[Pd^{II}{}_2Na_2KAs_4W_{40}O_{140}(H_2O)]^{21-}$ [19]. In 2021, Kato's group reported on the grafting of mono- and dipalladium(II) complexes on the monolacunary Keggin ion, $[\alpha\text{-}PW_{11}O_{39}\{Pd^{II}(Me_2ppz)\}]^{5-}$ and $[\alpha\text{-}PW_{11}O_{39}\{Pd^{II}(en)\}_2]^{3-}$ [20]. In 2024 Zheng reported on the fusion of a cyclic $Te^{IV}{}_3(Pd^{II}(SO_3)_2)_3$ unit with a $Te^{IV}W_6$ ion [21]. To date, no example of a structurally characterized high-valent $Pd^{IV}$-containing polyoxotungstate is known. An earlier report by Hill's group (*JACS* **2005**, *127*, 11948–11949) was withdrawn in 2012. Herein, we present the first example of a structurally characterized palladium(IV)-containing polyoxotungstate.

## 1.1 | Synthesis and Structure

We have synthesized the first example of a palladium(IV)-containing polyoxotungstate, $[Pd^{IV}W_6O_{24}]^{8-}$ (**$PdW_6$**, see Figure 1), by reacting $Na_2WO_4$ with $(NH_4)_2Pd^{IV}Cl_6$ in aqueous, acidic solution using conventional conditions and mild heating [22]. The initial reaction mixture was stirred at room temperature for 5 min, and then the pH was adjusted to 6.5 using nitric acid. This solution was further heated for 30 min at 60°C, and then a color change to orange was observed, indicating the formation of **$PdW_6$**. The yield (23%) is modest but represents the best outcome based on optimized reaction conditions. The title polyanion can be prepared in the pH range 4.5–7.0, but the reported conditions resulted in the highest yield.

Single-crystal XRD revealed that **$PdW_6$** crystallizes as a hydrated sodium salt $Na_8[Pd^{IV}W_6O_{24}]\cdot 28H_2O$ (**Na-$PdW_6$**) in the monoclinic space group $P2_1/n$ [23]. The polyanion **$PdW_6$** contains an octahedrally-coordinated palladium(IV) ion surrounded by a six-membered tungsten(VI)-oxo ring, resulting in the Anderson–Evans structure type with idealized $D_3d$ symmetry. The $Pd^{IV}$ ion is coordinated to six $\mu_3$-oxo ligands with $Pd^{IV}$—O bond lengths in the range of 1.99(5)–2.00(5) Å (Table S1), whereas the six $W^{VI}$ ions in the surrounding ring are each coordinated by two $\mu_3$-oxo, two $\mu_2$-oxo, and two terminal oxo ligands with $W^{VI}$—O bond distances in the range of 2.13(5)–2.17(6) Å, 1.93(6)–1.98(6) Å, and 1.75(6)–1.77(6) Å, respectively. The oxidation state of the central palladium(IV) ion in **$PdW_6$** was confirmed by bond valence sum (BVS) calculations (see also Supporting Information), which also confirmed the absence of any protonation on the oxygen atoms [24, 25].

The IR spectrum of **Na-$PdW_6$** exhibits characteristic peaks of W═$O_t$ at 906 and 859 $cm^{-1}$, and the bands at 635, 581, and 473 can be attributed to W—O—W and W—O—$Pd^{IV}$ bonds (Figure S1). These vibrational features are consistent with earlier reports on other Anderson–Evans type ions such as $[H_3Cr^{III}W_6O_{24}]^{6-}$ [26], $[Sb^{V}W_6O_{24}]^{7-}$ [27], $[Te^{VI}W_6O_{24}]^{6-}$ [27], and $[I^{VII}W_6O_{24}]^{5-}$ [28]. Thermogravimetric analysis (TGA) of **Na-$PdW_6$** revealed an initial weight loss of 22% from room temperature to 120°C, corresponding to the loss of ca. 25 water molecules of crystallization (Figure S2).

In 2010, Angus–Dunne reported the palladium(IV)-containing hexamolybdate $[Pd^{IV}Mo_6O_{24}H_3]^{5-}$ with an Anderson–Evans-type structure as based on single-crystal XRD and XPS [29]. In 2023, our group reported a mixed-valence palladium(IV/II) oxoanion $[Pd^{IV}O_6Pd^{II}{}_6((O_2CH_3As)_2)_6]^{2-}$ comprising a central, octahedrally coordinated $Pd^{IV}$ ion surrounded by a ring of six square-planar coordinated $Pd^{II}$ ions that are capped by six dimethylarsinate (cacodylate) groups, resulting in a derivative of the classical Anderson–Evans structure [30].

In 2002, Uk Lee reported the hexatungstoplatinate(IV) $[H_3Pt^{IV}W_6O_{24}]^{5-}$, which is the $Pt^{IV}$-analogue of **$PdW_6$** and observed $Pt^{IV}$—O bond lengths in the range of 1.97(10)–2.01(10) Å, very similar to the $Pd^{IV}$—O bond lengths in **$PdW_6$** [31]. Already in 1984, Lee and Sasaki reported the molybdenum analogues $[\alpha\text{-}H_{4.5}Pt^{IV}Mo_6O_{24}]^{3.5-}$ and $[\beta\text{-}H_4Pt^{IV}Mo_6O_{24}]^{4-}$, respectively [32]. Other examples of tetravalent metal-centered derivatives of the Anderson–Evans structure type are $[Mn^{IV}W_6O_{24}]^{8-}$ [33], and $[HIr^{IV}W_6O_{24}]^{7-}$ [34].

## 1.2 | X-Ray Photoelectron Spectroscopy

Figure 2 shows the photoelectron spectrum and fits for **Na-$PdW_6$** (upper panel), the palladium(IV) reference compound $(NH_4)_2Pd^{IV}Cl_6$ (middle panel, this salt is also a reactant in the synthetic procedure of **$PdW_6$**), and the palladium(II) reference compound $K_2Pd^{II}Cl_4$ (lower panel). The spectrum of **Na-$PdW_6$**

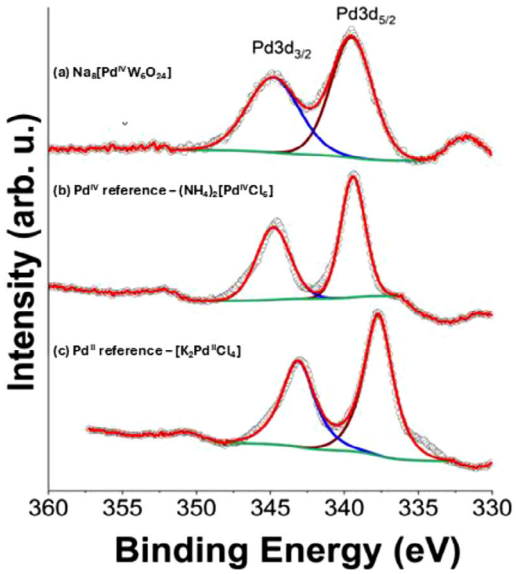


**FIGURE 2** | X-ray photoelectron spectra of **Na-Pd$^{IV}$W$_6$** (upper) and the reference compounds $(NH_4)_2Pd^{IV}Cl_6$ (middle) and $K_2Pd^{II}Cl_4$ (bottom), respectively.

exhibits two peaks related to Pd $3d_{5/2}$ and $3d_{3/2}$ core energy levels at the binding energies of 339.5 and 344.8 eV, respectively. These measured values are attributed to a +4 oxidation state of palladium in **PdW$_6$**, fully consistent with the data for the $Pd^{IV}$ reference compound $(NH_4)_2Pd^{IV}Cl_6$. On the other hand, the spectrum of the palladium(II) reference compound $K_2Pd^{II}Cl_4$ shows peaks at 337.5 and 342.6 eV ($Pd3d_{5/2}$ and $3d_{3/2}$, respectively), which are characteristic of Pd in the +2-oxidation state. The XPS data confirm that **PdW$_6$** contains a palladium ion in the +4 oxidation state.

## 1.3 | Hydrogenation Catalysis

The catalyst performance in the hydrogenation of *o*-xylene to *cis*-/-*trans*-1,2-dimethylcyclohexane (1,2-DMCH) was evaluated in a temperature sequence from 150°C to 370°C (20°C steps) under 28 bar $H_2$ with a 0.05 mL/min flow rate of *o*-xylene (see Scheme 1). The polyanion **PdW$_6$** was immobilized at 1 wt% on mesoporous SBA-15 functionalized with aminopropyltriethoxysilane (apts), followed by thermal activation at 400°C for 5 h (1°C/min ramp). For all catalytic runs, 450 mg of the calcined $PdW_6$-SBA-15-apts was used, carefully pelletized, crushed, and sieved to a 40–60 mesh particle size. To ensure proper thermal conductivity and flow behavior within the fixed-bed reactor, 11 g of silicon carbide (SiC, 120 grit) was loaded at the base of the reactor tube, followed by the addition of ~3 g of SiC, which was layered above to confine the catalyst and maintain consistent gas dispersion. The reactor was packed such that the thermocouple tip was precisely embedded in the catalyst zone, enabling accurate, real-time temperature monitoring under dynamic reaction conditions.

As shown in Figure 3a, the conversion increased steadily, reaching a maximum of 70% at 310°C–370°C. The *cis/trans* product distribution revealed a classic kinetic thermodynamic switch: *cis*-1,2-DMCH was favored at lower temperatures (70% *cis*-1,2-DMCH at 150°C), whereas *trans*-1,2-DMCH became dominant above 270°C, reaching 75% at 310°C–370°C (see Figure 3a). This temperature-dependent *cis*/*trans* distribution is consistent with reported arene hydrogenation behavior, where product stereochemistry is affected by reaction temperature and hydrogenation conditions [35, 36]. In this study, $PdW_6$-SBA-15-apts is described as a precatalyst for the hydrogenation reaction. This terminology is consistent with our previous reports in which discrete polyoxopalladates(II) and $Pd^{II}$-containing polyoxotungstates were used as discrete precursors to supported Pd-based nanoparticles for heterogeneous arene hydrogenation, including *o*-xylene hydroconversion [36, 37]. The structural evolution and catalytic role of the tungsten-oxo caps under the hydrogenation conditions remain to be determined in future studies.

To assess the influence of residence time, the catalyst was evaluated at 310°C in a series of increasing *o*-xylene flow rates (0.05–0.40 mL/min). As detailed in Figure 3b, conversion decreased progressively from 70% to 22%, confirming the crucial role of contact time in enabling full hydrogenation. Product selectivity remained largely unaffected under high-flow conditions, indicating that thermodynamic control dominates at elevated temperatures, regardless of residence time. Furthermore, the catalyst was subjected to five consecutive reaction cycles under standard conditions (310°C, 0.05 mL/min) without any significant decline in activity or selectivity, see Figure 3c, underscoring its structural robustness and reusability.

## 1.4 | Electrochemistry

The electrochemical behavior of **Na-PdW$_6$** was investigated in aqueous media at pH 6.5 and pH 2.0 by using cyclic voltammetry (CV). A solid sample of **Na-PdW$_6$** was immobilized on the basal plane of a pyrolytic graphite disk (PGB), and its response was evaluated either in a pH 6.5 solution (0.5 M $Na_2SO_4$) or in an acidic buffer (pH 2.0, 0.5 M $Na_2SO_4$ + $H_2SO_4$). Figure 4A presents the CVs of **Na-PdW$_6$** recorded at 100 mV·s$^{-1}$ within the potential window of +0.50 V to –1.20 V versus SCE at pH 6.5. The voltammogram reveals three distinct reduction processes (peaks I, II, and III), which can be assigned to the $Pd^{IV/II}$, $Pd^{II/0}$, and $W^{VI/V}$ couples, respectively, at −0.292, −0.535, and −1.084 V versus SCE. The peak-to-peak separation ($\Delta E_p$) for the first reduction step (peak I) is 59 mV at 0.1 V·s$^{-1}$, consistent with a rapid electron transfer. The second reduction corresponds to the $Pd^{II} \rightarrow Pd^0$ process, and the final reduction is associated with the tungsten centers, both being irreversible. As illustrated in the inset of Figure S3, the current intensities of the first reduction scale linearly with the scan rate, which is characteristic of a surface-confined redox process. Importantly, successive CV scans confirmed that **PdW$_6$** remains stable upon reduction at this initial stage (peak I). For comparison, CV experiments performed with a $Pd^{II}SO_4$ reference solution under the same conditions produced similar reduction features, consistent with the irreversible conversion of $Pd^{II}$ to metallic $Pd^0$. During the reverse scan for $Pd^{II}SO_4$, an additional anodic signal emerged near −0.12 V versus SCE, attributable to the oxidative dissolution of $Pd^0$. This observation indicates that the irreversible $Pd^{II} \rightarrow Pd^0$ reduction is accompanied by partial decomposition of **PdW$_6$**.

At lower pH, the polyanion **PdW$_6$** is less stable, as shown in Figure 4B. The CVs recorded at pH 2 closely resemble those of

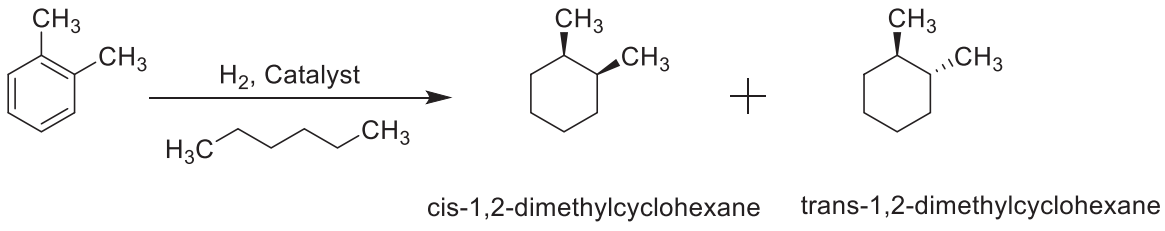


**SCHEME 1** | Hydrogenation of *o*-xylene to *cis*- and *trans*-1,2-dimethylcyclohexane using $PdW_6$-SBA-15-apts as precatalyst under $H_2$ pressure.

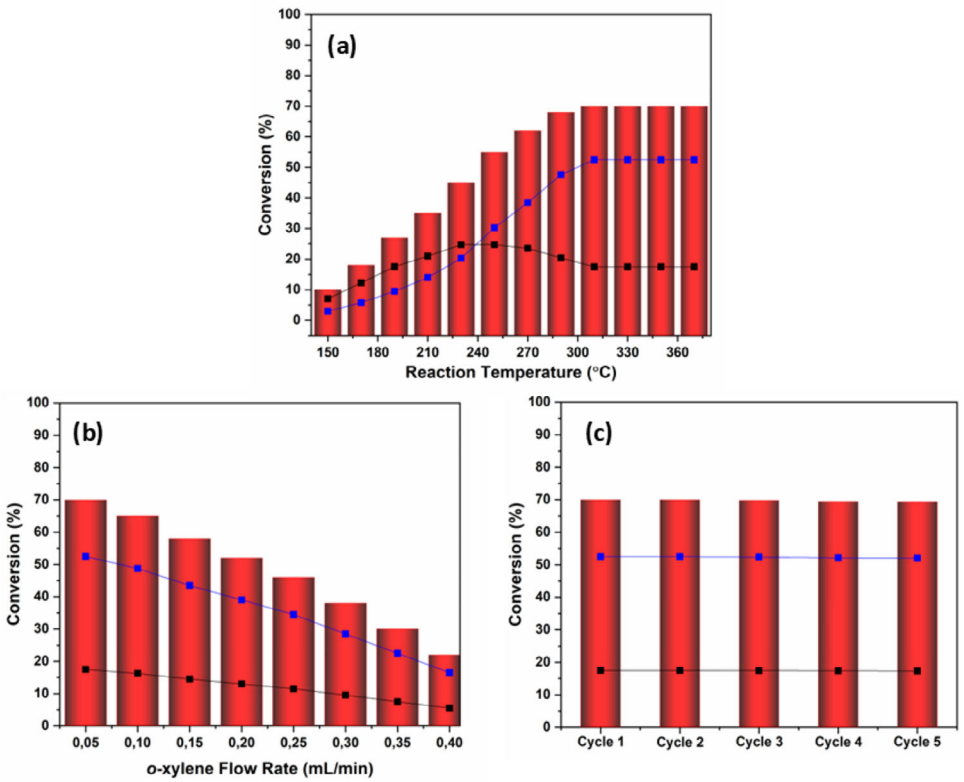


**FIGURE 3** | (a) Hydroconversion of *o*-xylene to 1,2-DMCH at various reaction temperatures using $PdW_6$-SBA-15-apts as precatalyst. Conditions: 28 bar $H_2$, flow rate 0.05 mL/min. The curves represent the percentage of *cis*-1,2-DMCH (black) and *trans*-1,2-DMCH (blue) isomers of 1,2-DMCH in the product. (b) Hydroconversion of *o*-xylene to 1,2-DMCH under varying substrate flow rates using $PdW_6$-SBA-15-apts as precatalyst. The curves represent the percentage of *cis*-1,2-DMCH (black) and *trans*-1,2-DMCH (blue) isomers of 1,2-DMCH in the product. Reaction conditions: 310°C, 28 bar $H_2$. (c) Catalytic stability of $PdW_6$-SBA-15-apts in the hydroconversion of o-xylene to 1,2- DMCH. The curves represent the percentage of *cis*-1,2-DMCH (black) and *trans*-1,2-DMCH (blue) isomers of 1,2-DMCH in the product. Reaction conditions: 310°C, 28 bar $H_2$, flow rate 0.05 mL/min.

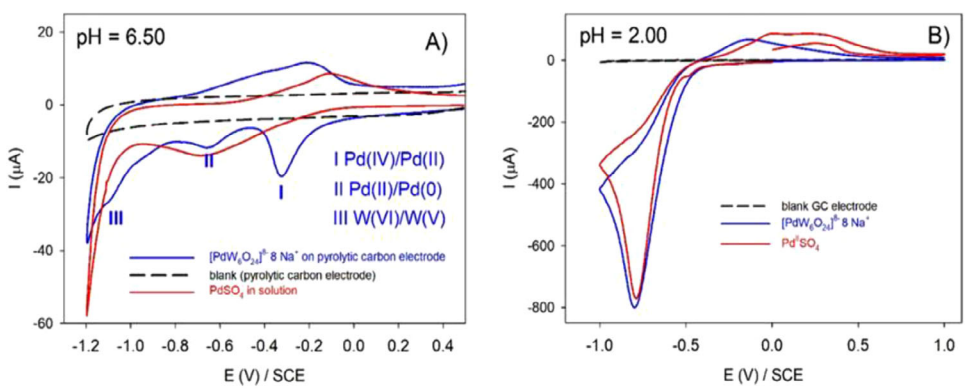


**FIGURE 4** | Cyclic voltammograms of **Na-PdW$_6$** immobilized on a PGB electrode ($d = 2$ mm), (A) in a 0.5 M $Na_2SO_4$ solution (pH 6.5) and (B) in a 0.5 M pH 2.0 $H_2SO_4$–$Na_2SO_4$ buffer solution. Scan rate: 100 mV $s^{-1}$. Red curve: CVs of 0.3 mM of $Pd^{II}SO_4$ solution measured at pH 6.5 and pH 2.0 using a glassy carbon electrode (Ø = 3 mm).

$Pd^{II}SO_4$, indicating decomposition of **$PdW_6$** and the release of Pd species in the form of $Pd^{II}$ ions.

## 2 | Conclusions

We have synthesized the first palladium(IV)-containing polyoxotungstate, $[Pd^{IV}W_6O_{24}]^{8-}$ (**$PdW_6$**), via a simple one-pot procedure in aqueous acidic medium. The polyanion **$PdW_6$** comprises a central, 6-coordinated $Pd^{IV}$ ion surrounded by six edge-shared $WO_6$ octahedra. The sodium salt of **$PdW_6$** was characterized in the solid state by single-crystal and powder XRD, FT-IR, TGA, and elemental analysis. The +4 oxidation state of the central Pd ion in **$PdW_6$** was confirmed by X-ray photoelectron spectroscopy (XPS). The solution electrochemistry was investigated by cyclic voltammetry (CV), and also confirmed the existence of $Pd^{IV}$ in **$PdW_6$**, which can be reduced reversibly to $Pd^{II}$. We also immobilized **$PdW_6$** on apts-modified SBA-15 support as a precatalyst and observed notable catalytic activity, achieving ~70% conversion of *o*-xylene to *cis*/*trans* 1,2-dimethylcyclohexane. In future work, we aim to expand upon this work by using other noble metals.


### Acknowledgments

Open access funding enabled and organized by Projekt DEAL.

U.K. thanks the German Research Council (DFG, KO-2288/29-1, KO-2288/31-1, and KO-2288/33-1) and Constructor University for support. L.R. and S.D. thank the University of Strasbourg and the CNRS, as well as the Foundation Jean-Marie Lehn and the ITI CSC (chemistry of complex systems).


### Conflicts of Interest

The authors declare no conflicts of interest.

### Data Availability Statement

The data that support the findings of this study are available in the Supporting Information of this article.

### References


1. M. T. Pope, *Heteropoly and Isopoly Oxometalates* (Springer-Verlag, 1983), https://doi.org/10.1007/978-3-662-12004-0.

2. V. W. Day and W. G. Klemperer, "Metal Oxide Chemistry in Solution: The Early Transition Metal Polyoxoanions," *Science* 228 (1985): 533–541, https://doi.org/10.1126/science.228.4699.533.

3. M. T. Pope and A. Müller, "Polyoxometalate Chemistry: An Old Field With New Dimensions in Several Disciplines," *Angewandte Chemie International Edition in English* 30 (1991): 34–48, https://doi.org/10.1002/anie.199100341.

4. C. L. Hill, guest ed., issue dedicated to Polyoxometalates, *Chemical Reviews* 98 (1998): 1–390, https://pubs.acs.org/toc/chreay/98/1.

5. P. Yang and U. Kortz, 7.02 Quo Vadis, Polyoxometalate Chemistry? in *Comprehensive Coordination Chemistry III* ed. E. C. Constable, G. Parkin, and L. Que Jr., 7 (Elsevier, 2021): 4–28, https://doi.org/10.1016/B978-0-08-102688-5.00065-9.

6. L.-L. Liu, L. Wang, X.-Y. Xiao, P. Yang, J. Zhao, and U. Kortz, "Structural Overview and Evolution Paths of Lacunary Polyoxometalates," *Coordination Chemistry Reviews* 506 (2024): 215687–215715, https://doi.org/10.1016/j.ccr.2024.215687.

7. N. V. Izarova, M. T. Pope, and U. Kortz, "Noble Metals in Polyoxometalates," *Angewandte Chemie International Edition* 51 (2012): 9492–9510, https://doi.org/10.1002/anie.201202750.

8. P. Yang and U. Kortz, "Discovery and Evolution of Polyoxopalladates," *Accounts of Chemical Research* 51 (2018): 1599–1608, https://doi.org/10.1021/acs.accounts.8b00082.

9. S. J. Angus-Dunne, R. C. Burns, D. C. Craig, and G. A. Lawrance, "A Novel Heteropolymetalate Containing Palladium(II): Synthesis and Crystal Structure of $K_2Na_6[Pd_2W_{10}O_{36}]\cdot 22H_2O$," *Journal of the Chemical Society, Chemical Communications* 4 (1994): 523–524, https://doi.org/10.1039/C39940000523.

10. L.-H. Bi, U. Kortz, B. Keita, L. Nadjo, and H. Borrmann, "Palladium(II)-Substituted Tungstosilicate $[Cs_2K(H_2O)_7\text{-}Pd_2WO(H_2O)(A\text{-}\alpha\text{-}SiW_9O_{34})_2]^{9-}$," *Inorganic Chemistry* 43 (2004): 8367–8372, https://doi.org/10.1021/ic048864z.

11. L.-H. Bi, M. Reicke, U. Kortz, B. Keita, L. Nadjo, and R. J. Clark, "The First Structurally Characterized Palladium(II)- Substituted Polyoxoanion: $[Cs_2Na(H_2O)_{10}Pd_3(\alpha\text{-}Sb^{III}W_9O_{33})_2]^{9-}$," *Inorganic Chemistry* 43 (2004): 3915–3920, https://doi.org/10.1021/ic049736d.

12. L.-H. Bi, U. Kortz, B. Keita, L. Nadjo, and L. Daniels, "The Palladium(II)-Substituted, *Lone Pair Containing Tungstoarsenates*(III) $[Na_2(H_2O)_2PdWO(H_2O)(\alpha\text{-}AsW_9O_{33})_2]^{10-}$ and $[Cs_2Na(H_2O)_8Pd_3(\alpha\text{-}AsW_9O_{33})_2]^{9-}$," *European Journal of Inorganic Chemistry* 2005 (2005): 3034–3041, https://doi.org/10.1002/ejic.200500128.

13. L.-H. Bi, M. H. Dickman, and U. Kortz, "The Palladium(II)-Decorated 22-Tungsto-2-Bismuthate(III), $[Pd_3(H_2O)_9Bi_2W_{22}O_{76}]^{8-}$," *CrystEngComm* 11 (2009): 965–966, https://doi.org/10.1039/B820888C.

14. N. V. Izarova, A. Banerjee, and U. Kortz, "Noble Metals in Polyoxometalate Chemistry: Palladium-Containing Derivatives of the Monolacunary Keggin and Wells-Dawson Tungstophosphates," *Inorganic Chemistry* 50 (2011): 10379–10386, https://doi.org/10.1021/ic201451x.

15. J. Gao, J. Yan, S. Beeg, D.-L. Long, and L. Cronin, "Assembly of Molecular "Layered" Heteropolyoxometalate Architectures," *Angewandte Chemie International Edition* 51 (2012): 3373–3376, https://doi.org/10.1002/anie.201108428.

16. N. V. Izarova, R. I. Maksimovskaya, S. Willbold, and P. Kögerler, "Tetrapalladium-Containing Polyoxotungstate $[Pd^{II}_4(\alpha\text{-}P_2W_{15}O_{56})_2]^{16-}$: A Comparative Study," *Inorganic Chemistry* 53 (2014): 11778–11784, https://doi.org/10.1021/ic502080x.

17. A. Rajan, A. S. Mougharbel, S. Bhattacharya, T. Nisar, V. Wagner, and U. Kortz, "Palladium(II)-Containing Tungstoarsenate(V), $[Pd^{II}_4(As_2W_{15}O_{56})_2]^{16-}$, and Its Catalytic Properties," *Inorganic Chemistry* 59 (2020): 13042–13049, https://doi.org/10.1021/acs.inorgchem.0c01737.

18. N. V. Izarova, B. Santiago-Schübel, S. Willbold, V. Heß, and P. Kögerler, "Classical/Non-Classical Polyoxometalate Hybrids," *Chemistry—A European Journal* 22 (2016): 16052–16056, https://doi.org/10.1002/chem.201604238.

19. Z. Lin, N. V. Izarova, F. T. Mehari, and U. Kortz, "Palladium(II) Incorporation in the All-Inorganic Cryptand $[As_4W_{40}O_{140}]^{28-}$: Synthesis and Structural Characterization of $[Pd_2Na_2KAs_4W_{40}O_{140}(H_2O)]^{21-}$," *Zeitschrift für Anorganische und Allgemeine Chemie* 644 (2018): 1379–1382, https://doi.org/10.1002/zaac.201800327.

20. C. N. Kato, I. Nakahira, R. Kasai, and S. Mori, "Syntheses, Molecular Structures, and Countercation-Induced Structural Transformation of Monomeric α-Keggin-Type Polyoxotungstate-Coordinated Mono- and Dipalladium(II) Complexes," *European Journal of Inorganic Chemistry* 19 (2021): 1816–1827, https://doi.org/10.1002/ejic.202100075.

21. L. Jia, Y.-X. Liu, X. X. Li, C. Sun, and S.-T. Zheng, "A Palladium-Containing Polyoxotungstate With Anisotropic Proton Conductivity," *Inorganic Chemistry* 63 (2024): 14308–14312, https://doi.org/10.1021/acs.inorgchem.4c02447.

22. **Synthesis of $Na_8[Pd^{IV}W_6O_{24}]\cdot 28H_2O$ (Na-$PdW_6$)** $(NH_4)_2Pd^{IV}Cl_6$ (15 mg, 0.042 mmol) and $Na_2WO_4\cdot 2H_2O$ (150 mg, 0.455 mmol) were dissolved in 5 mL 0.5 M NaOAc solution (pH 6) and stirred for 5 minutes

at room temperature. Then the pH was adjusted to 6.5 using 0.15 M $HNO_3$ and the solution was further stirred at 60°C for 30 minutes, followed by filtration. The filtrate was kept in an open vial for crystallization. After several days, orange plate-shaped crystals of $Na_8[Pd^{IV}W_6O_{24}]\cdot 28H_2O$ (**Na-PdW$_6$**) together with colorless crystals of **Na-PdW$_6$** were observed. The crystals of **Na-PdW$_6$** were manually separated, as no synthetic condition leading to a pure product could be identified. Yield 22 mg (23%, based on Pd). FT-IR (KBr pellet, $cm^{-1}$) in the fingerprint region: 1640(s), 1565(sh), 1417 (w), 906(s), 859(s), 635(m), 574(m), 479(m), 431(w). Elemental analysis: Calcd (%) for **Na-PdW$_6$**: Pd, 4.6; W, 48.4; Na, 8.0 Found (%): Pd, 4.0; W, 49.6; Na, 7.5.

23. *Deposition number 2479164 for **Na-PdW$_6$** contains the supplementary crystallographic data for this paper. These data are provided free of charge by the joint Cambridge Crystallographic Data Centre and Fachinformationzentrum Karlsruhe Access Structures service.*


24. N. E. Brese and M. O'Keeffe, "Bond-Valence Parameters for Solids," *Acta Crystallographica Section B Structural Science* B47 (1991): 192–197, https://doi.org/10.1107/S0108768190011041.

25. I. D. Brown and D. Altermatt, "Bond-Valence Parameters Obtained From a Systematic Analysis of the Inorganic Crystal Structure Database," *Acta Crystallographica Section B Structural Science* 41 (1985): 244–247, https://doi.org/10.1107/S0108768185002063.

26. W. Liu, Z. Lin, B. S. Bassil, R. Al-Oweini, and U. Kortz, "Synthesis and Structure of Hexatungstochromate $[H_3Cr^{III}W_6O_{24}]^{6-}$," *Chimia* 69 (2015): 537–537, https://doi.org/10.2533/chimia.

27. M. H. Alizadeh and A. R. Salimi, "Density Functional Theory and Hartree–Fock Studies: Geometry, Vibrational Frequencies and Electronic Properties of Anderson-Type Heteropolyanion, $[XM_6O_{24}]^{n-}$ (X = $Te^{VI}$, $I^{VII}$ and M = $Mo^V$, $W^V$) and $[Sb^VW_6O_{24}]^{7-}$," *Spectrochimica Acta Part A: Molecular and Biomolecular Spectroscopy* 65 (2006): 1104–1111, https://doi.org/10.1016/j.saa.2006.02.011.

28. A. C. Dengel, W. P. Griffith, S. I. Mostafa, and A. J. P. White, "Raman and Infrared Study of Some Metal Periodato Complexes," *Spectrochimica Acta Part A: Molecular and Biomolecular Spectroscopy* 49 (1993): 1583–1589, https://doi.org/10.1016/0584-8539(93)80115-Q.

29. S. Angus-Dunne, R. C. Burns, D. C. Craig, and G. A. Lawrance, "Synthesis and Crystal Structure of the Palladium(IV) Polyoxomolybdate, $K_{0.75}Na_{3.75}[PdMo_6O_{24}H_{3.5}]\cdot 17H_2O$," *Zeitschrift für Anorganische und Allgemeine Chemie* 636 (2010): 727–734, https://doi.org/10.1002/zaac.200900129.

30. X. Ma, S. Bhattacharya, T. Nisar, et al., "Mixed-valent Palladium(IV/II)-Oxoanion, $[Pd^{IV}O_6Pd^{II}_6((CH_3)_2AsO_2)_6]^{2-}$," *Chemical Communications* 59 (2023): 904–907, https://doi.org/10.1039/D2CC05699B.

31. U. Lee, "Pentapotassium Trihydrogenhexatungstoplatinate(IV) Hexahydrate, $K_5[H_3PtW_6O_{24}]\cdot 6H_2O$," *Acta Crystallographica* E58 (2002): i130–i132, https://doi.org/10.1107/S1600536802021505.

32. U. Lee and Y. Sasaki, "Isomerism of the Hexamolybdo-Platinate(IV) Polyanion. Crystal structure of $K_{3.5}[\alpha\text{-}H_{4.5}Pt^{IV}Mo_6O_{24}]\cdot 3H_2O$ and $(NH_4)_4[\beta\text{-}H_4PtMo_6O_{24}]\cdot 1.5H_2O$," *Chemistry Letters* 13 (1984): 1297–1300, https://doi.org/10.1246/cl.1984.1297.

33. A. L. Nolan, R. C. Burns, G. A. Lawrance, and D. C. Craig, "Octasodium Hexatungstomanganate(IV) Octadecahydrate," *Acta Crystallographica* 56 (2000): 729–730, https://doi.org/10.1107/S010827010000408X.

34. S. A. Adonin, N. V. Izarova, C. Besson, et al., "An $Ir^{IV}$-Containing Polyoxometalate," *Chemical Communications* 51 (2015): 1222–1225, https://doi.org/10.1039/C4CC09271F.

35. M. P. Wiesenfeldt, Z. Nairoukh, T. Dalton, and F. Glorius, "Selective Arene Hydrogenation for Direct Access to Saturated Carbo- and Heterocycles," *Angewandte Chemie International Edition* 58 (2019): 10460–10476, https://doi.org/10.1002/anie.201814471.

36. P. Yang, M. E. Mahmoud, Y. Xiang, et al., "Host–Guest Chemistry in Discrete Polyoxo-12-Palladate(II) Cubes $[MO_8Pd_{12}L_8]^{n-}$: Structure, Magnetism, and Catalytic Hydrogenation," *Inorganic Chemistry* 61 (2022): 18524–18535, https://doi.org/10.1021/acs.inorgchem.2c02751.

37. W. W. Ayass, J. F. Miñambres, P. Yang, et al., "Discrete Polyoxopalladates as Molecular Precursors for Supported Palladium Metal Nanoparticles as Hydrogenation Catalysts," *Inorganic Chemistry* 58 (2019): 5576–5582, https://doi.org/10.1021/acs.inorgchem.8b03513.


## Supporting Information

Additional supporting information can be found online in the Supporting Information section.

**Supporting File**: The Supporting Information is available at https://doi.org/10.1002/chem.71182.